Nano World Journal

https://doi.org/10.17756/nwj.2023-s3-052

Research Article

Open Access

A Basic Confirmational Study of Copper(I) Oxide Nanoparticles by Varying Molar Ratio for the Current Applications

Annai Delphin Charles[1,2], Arunachalan Prabakaran[2*] and Pauline Vijay Muthu[2]

[1]Department of Physics College Name – Bon Secours Arts and Science College for Women (Affiliated to Mother Teresa Women's University, Kodaikanal), Dindigul, Tamil Nadu, India

[2]Department of Physics, Vel Tech Rangarajan Dr. Sagunthala R&D Institute of Science and Technology, Chennai, Tamil Nadu, India

***Correspondence to:**
Arunachalan Prabakaran
Department of Physics,
Vel Tech Rangarajan Dr. Sagunthala R&D Institute of Science and Technology,
Chennai, Tamil Nadu, India.
E-mail: draprabakaran@veltech.edu.in

Received: July 27, 2023
Accepted: October 06, 2023
Published: October 10, 2023

Citation: Charles AD, Prabakaran A, Muthu PV. 2023. A Basic Confirmational Study of Copper(I) Oxide Nanoparticles by Varying Molar Ratio for the Current Applications. *NanoWorld J* 9(S3): S267-S272.

Copyright: © 2023 Charles et al. This is an Open Access article distributed under the terms of the Creative Commons Attribution 4.0 International License (CCBY) (http://creativecommons.org/licenses/by/4.0/) which permits commercial use, including reproduction, adaptation, and distribution of the article provided the original author and source are credited.

Published by United Scientific Group

Abstract

Current applications are emerging in conductive applications and optical devices fabrication and biological applications. Pristine copper(I) oxide (Cu_2O) nanoparticles were synthesized and characterized through FE-SEM (Field emission-scanning electron microscope), XRD (X-ray diffraction), FTIR (Fourier transform infrared spectroscopy). Cu_2O nanoparticles are compared by varying molar ratios. The properties and nature of Cu_2O nanoparticles were enhanced with an increase of molar ratio. Enhancement in properties helps in developing energy applications. Prepared Cu_2O nanoparticles for development in bio applications and energy storage device. FE-SEM reveals that prepared nanoparticles lie within the range of 15 - 295 nm depending upon corresponding molar ratios. Which also proposes the nano regime. Other studies XRD, UV-Vis DRS (Ultraviolet-Visible Diffuse Reflectance Spectroscopy), FTIR study reveals the pristine nature of Cu_2O.

Keywords

Nanoparticles, Copper(I) oxide, Characterization studies

Introduction

The world of nanotechnology emerges with the evolution of producing materials at the nano scale which reduces the complexity through miniaturization. Nanomaterials help with their enhanced and unique properties such as structural, optical, magnetic properties without changing their original compound structure and nature. The conversion of nanomaterials from bulk nature enhances and modifies the physical and mechanical properties of the materials which help in various applications such as electrochemical devices, biological applications, sensors, wastewater treatment [1, 2]. With respect to bottom-up and top-down approaches there are several important methods that are popular for their production of nanomaterials with unique physical and chemical properties. Among various methods such as sol-gel, co-precipitation, solid-state reaction, ball milling, alkoxide-based synthesis, Sono chemical preparation, microwave irradiation, and thermal decomposition [3], chemical methods like sol-gel, and co-precipitation are mostly used methods and environmentally friendly and cost-effective [4]. For those proposed methods metal oxides such as TiO_2, ZnO, CuO, Cu_2O, Co_3O_4, Fe_3O_4, and Fe_2O_4 are being synthesized for various applications. Among these metal oxides, Cu_2O has unique properties such as catalytic properties, biological properties, magnetic properties, enhanced electronic transitions with doping of other metal and metal oxides. These modifications are well executed in the applications of battery storages, magnetic media, super conductors, sensors, and mechanical devices, etc. [5, 6].

In the economic world, the field of mining earth elements in western countries is increasing and also increases the economy globally. Metal copper mining has decreased due to the long-term process of getting copper from copper sulfides [7]. This makes an attraction Cu_2O due to its stability and is complex and stable compositions [8, 9].

The present study focuses on synthesis of Cu_2O nanoparticles and claims the basic study about Cu_2O nanoparticles. We have synthesized Cu2O nanoparticles for various applications and their morphological, structural changes depending upon precursor reducing agent's molar ratio were discussed. Every method of synthesis of Cu_2O nanoparticles explains how the properties were changed, but the interaction mechanisms were not explained in recent approaches, we determine the possibility of interaction mechanisms and reduction mechanisms. Simply speaking, the possible reactions for product formations. And we explored some applications. In this work we explained the change of properties depending upon the structure formation of Cu_2O nanoparticles.

Materials and Method

Materials and synthesis

Copper acetate, glacial acetic acid, and sodium hydroxide pellets were purchased for the synthesis of Cu_2O nanoparticles. 1 M of copper acetate is dissolved in 50 ml of deionized water and made as a clear solution. During stirring the solution is heated at 70 °C then 2 ml of glacial acetic acid were added to the solution. Further stirring and heating at 70 °C - 80 °C, NaOH solution of 50 ml for various molar ratio were added dropwise and continuous stirred for 2 - 3 h a brown-black precipitate was obtained. After the precipitate formed, precipitate washed with water and ethanol for several times and dried at 90 °C for one hour. Obtained dried precipitate was calcined at 300 °C. Obtained product was grinded in mortar and pestle. Samples were prepared by varying the NaOH molar as 1, 2, 3 and named as C1, C2, C3. The sample details and sample codes are listed in table 1 and the scheme was illustrated in figure 1.

Depending upon increase in Na and Cu ratios precipitation showed color variance from greyish, to brownish and blackish brown for the samples C1, C2, C3 respectively. The reaction between copper(II) acetate and sodium hydroxide in

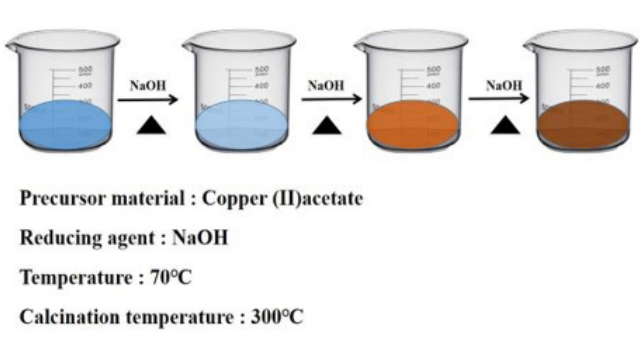


Figure 1: Scheme of Cu_2O nanoparticles.

Table 1: Sampler name index.

S. No.	Precursor: Reducing agent ration (Molar (M))	Sample code
1	1:1	C1
2	1:2	C2
3	1:3	C3

the presence of glacial acetic acid is likely the following equation 1.

$$Cu(C_2H_3O_2)_2\ (aq) + 2\ NaOH\ (aq) + 2CH_3COOH\ (aq) \rightarrow Cu(OH)_2\ (s) + 2CH_3COONa\ (aq) + 2H_2O \quad (1)$$

This reaction produces solid copper hydroxide along with sodium acetate (CH_3COONa) and water. The empirical formula for this reaction can be written as:

$$Cu(C_2H_3O_2)_2 + 2NaOH + 2CH_3COOH \rightarrow Cu(OH)_2 + 2CH_3COONa + 2H_2O \quad (2)$$

Calcination of copper hydroxide ($Cu(OH)_2$) at 300 °C can produce Cu_2O. In this case, the copper hydroxide is heated to a high enough temperature to drive off the water molecule and form Cu_2O. The reaction can be written as:

$$Cu(OH)_2\ (s) \rightarrow Cu_2O\ (s) + H_2O\ (g) \quad (3)$$

So, the final product of calcination of copper hydroxide is Cu_2O.

Instrumentation techniques

The morphological measurements of the Cu_2O nanoparticles have been made using FE-SEM of model CARL ZEISS, USA. The XRD patterns have been recorded by X-ray diffractometer of model Panalytical/Xpert 3. FTIR spectra have been obtained using Infrared spectrometer Spectrum 100, Perkin Elmer. The optical properties have been studied by UV-Vis DRS, employing spectrometer of model SHIZMADZU UV-2600.

Results and Discussion

SEM analysis

FE-SEM is used to determine the surface morphologies of Cu_2O nanoparticles. Cu_2O nanoparticles were scanned by varying the resolution for 100 nm, 1 µm, and 50 nm. FE-SEM images of three samples of Cu_2O nanoparticles were compared corresponding resolution 1 micron, 200 nm, and 100 nm. Precipitation influences the formation of morphology of Cu_2O nanoparticles. The highest ratio sample C3 was not highly dispersed and formed in microparticles because of increase in Na/Cu ratio. Na/Cu ratio facilitates immediate precipitation by the higher rate of nucleation due to increase in concentration of Na ions. Increase in concentration leads to immediate precipitation which affects morphology to form a cluster with maximum atomic attraction and minimum repulsion or higher aggregated particles. Here attraction and repulsion we meant that ionic strength of a solution or precipitate. While other samples C1 and C2 showed morphology that having micro-sized cubic clusters which are inhomogeneous with the smaller spherical shaped nanosized particles. Still, it is in nano

regime because of higher dispersion and repulsion rate. C1 has a cubic morphology with an average cube size of 261 nm with their smaller aggregates in the range of 17 nm - 46 nm (average size 28 nm) at 100 nm magnification. C2 indicates intermediate stage of transforming into cubes from smaller spherical aggregates morphology. Aggregated particles range from 27 nm - 140 nm with an average size of 52 nm. C3 has island morphology which spread like sand and formed micro-sized particles in the range of 55 nm - 296 nm with an average size of 99 nm. From morphology studies we have inferred that the formation of precipitation affects the morphology with respect to increase in molar ratios. Current work is evident that size of nanoparticles is increasing with increase in molar ratio. Figure 2 indicates the morphology of Cu_2O nanoparticles and size details given in table 2. Morphology itself confirms the formation of Cu_2O nanoparticles which provides cubical and spherical morphologies with smaller aggregation [10].

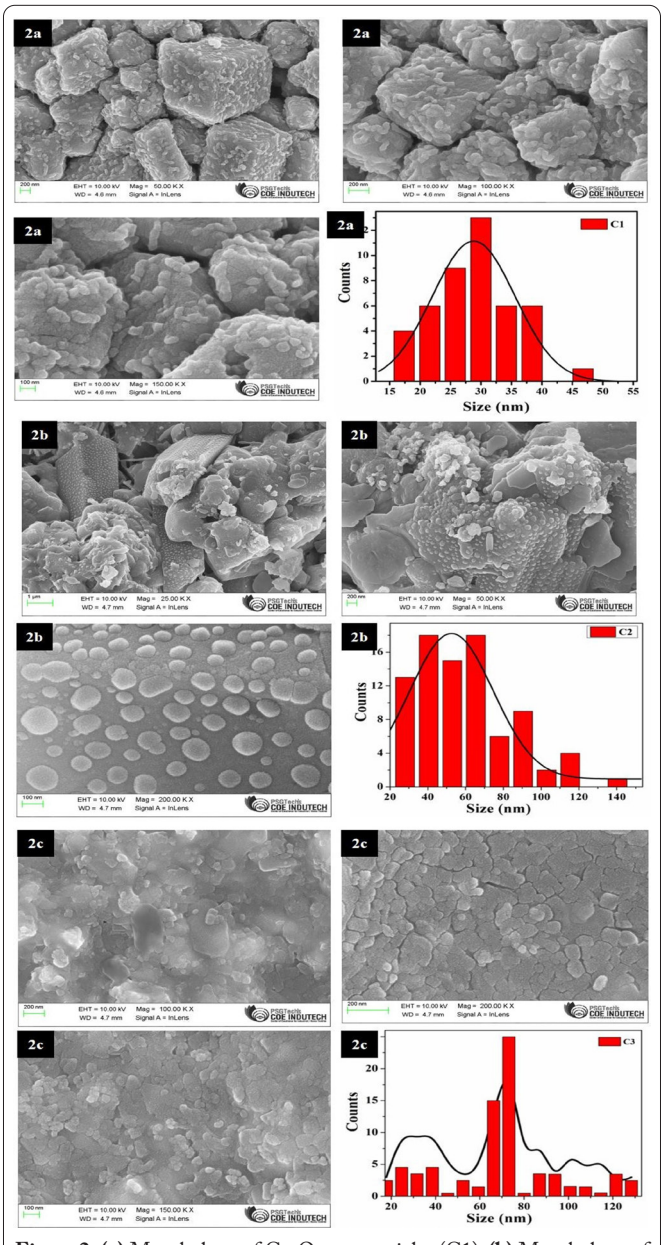


Figure 2: (a) Morphology of Cu_2O nanoparticles (C1), **(b)** Morphology of Cu_2O nanoparticles (C2), and **(c)** Morphology of Cu_2O nanoparticles (C3).

XRD analysis

Structural parameters of Cu_2O nanoparticles were determined by XRD analysis. XRD gives structural information such as crystallite size, lattice strain, lattice stress, and crystalline nature of the sample. Crystal structures determined by XRD analysis in the angle of 20° - 90°.The XRD pattern of the prepared Cu_2O nanoparticles is shown in figure 3a and the calculated values of the major structural parameters obtained from the XRD data are listed in table 3. The well-defined XRD peaks confirm the crystalline nature of the prepared Cu_2O nanoparticles corresponding to the Cubic Pn-3m space group. The crystal planes corresponding to the XRD peaks are located around 29°, 36°, 38°, 42°, 51°, 62°, 74° are indexed as (011), (111), (002), (002), (20-2), (022), (113), respectively and matches with JCPDS card number 98-006-0704 [11]. The crystallite size of the sample calculated using Debye-Scherer formula and tabulated in table 3. The lattice strain (ε) has been calculated using the following formula and the symmetry pa-

Table 2: Particle size.

Sample code	Morphology	Range (nm)	Average size (nm)
C1	Cube	17 - 46	28
C2	Cube with spheres	27 - 140	52
C3	Sand like morphology	55 - 296	98

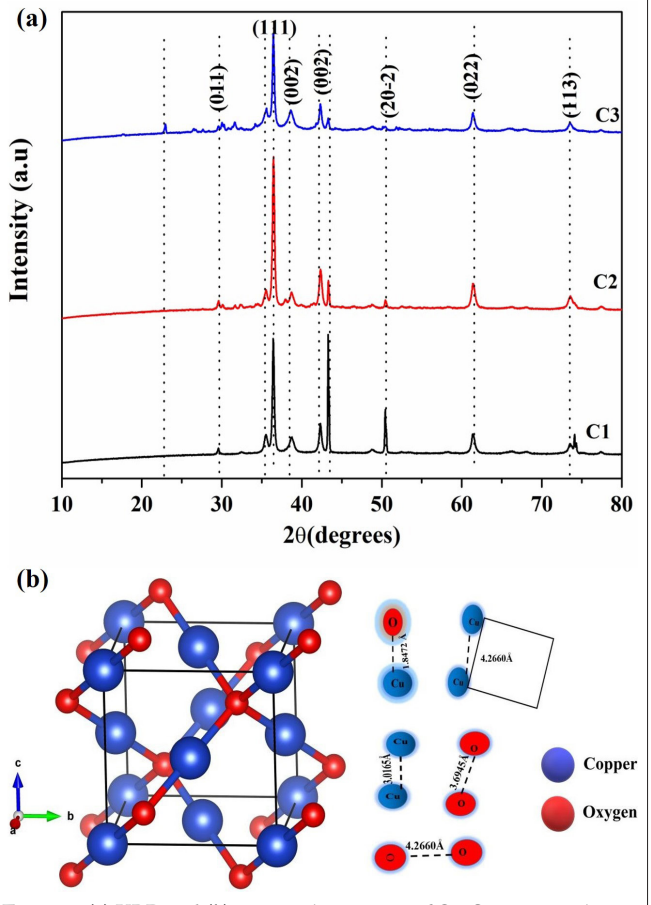


Figure 3: (a) XRD and **(b)** structural properties of Cu_2O nanoparticles.

Table 3: Structural properties of Cu_2O nanoparticles.

Sample code	Crystallite size (nm)	Dislocation density (X10^{-3} nm^{-2})	Lattice strain	Unit cell volume (Å^3)
C1	27.92	0.0012	0.00385	77.635882
C2	25.55	0.0015	0.0045	77.739672
C3	23.16	0.0018	0.0050	77.745144

Table 4: Lattice parameters and symmetries of Cu_2O nanoparticles.

Sample code	a = b = c (Å)	Phase α = β = γ (°)	Symmetry
C1	4.2660	90	Cu -3m O -43m
C2	4.26790	90	
C3	4.26800	90	

rameters are also tabulated in table 3 and table 4.

$$\varepsilon = \frac{\beta}{4\tan(\theta)} \quad (4)$$

$$D = \frac{k\lambda}{\beta\cos(\theta)} \quad (5)$$

In equation 4 represents the lattice strain and in equation 5, 'β' represents full width half maxima. The crystal structure of the prepared Cu_2O nanoparticles obtained from Rietveld analysis and the refined structure was visualized using VESTA software and illustrated in figure 3b. Bond length between atoms is studied using VESTA software which was matched with previous reports [12]. Bond length between diagonal copper atoms, diagonal oxygen atoms, copper atoms which are present in edges of the crystal, parallel plane oxygen atoms, Cu-O atoms were found and illustrated in figure 3b. Bond length values are tabulated in table 4. The values of the lattice constants, determined from the XRD data for the prepared cubic Cu_2O nanoparticles, were calculated. Size of crystallite decreases with an increase of concentration due to attraction between molecules and bond length between atoms were increased with an increase of Na concentrations. XRD studies reveal that the precipitation facilitates and extends the particles to the larger grains. Increase in concentrations also enhances the ionic strength and bonding between atoms.

FTIR analysis

Functional groups in the sample are determined by FTIR spectroscopy. Functional groups such as decomposition groups are present in the material. FTIR gives information about bonding of functional group of Cu_2O nanoparticles (Table 5). According to the FTIR analysis, abundant functional groups were present on the sample. It can be seen from figure 4 that all curves displayed a wide broad peak near 3500 - 2500 cm^{-1}, which was assigned to O–H bonded hydroxyl groups stretching vibration. Strong characteristic peak of Cu–O stretching vibration at 629 cm^{-1}, which indicates the presence of pure Cu_2O. The peak is around 1040 cm^{-1}, one singlet at 870 cm^{-1}, doublet at 1410 and 1330 cm^{-1} and another doublet at 760 and 700 cm^{-1}. These peaks indicate the presence of formation and C-H-N bonding's from the precursor. Peak variation from 2800 - 1700 cm^{-1} indicates the modification in ionic strength caused by the Na concentration. Ionic strength or bond length were stabilized by increase in Na concentration from C1 - C3 [13, 14].

UV-Vis DRS analysis

Optical properties studied using DRS technique. Band gaps were determined from reflectance using Kubelka–Munk function F(R). Using bandgap values, we have calculated some theoretical values such as refractive index and dielectric constant. These calculations help in improving ideas in fabrication of opto-electronic devices. Kubelka–Munk function F(R) equation as given below.

$$F(R) = K/S \text{ ratio} = (1-R)\ 2/2R \quad (6)$$

Where, R is reflectance.

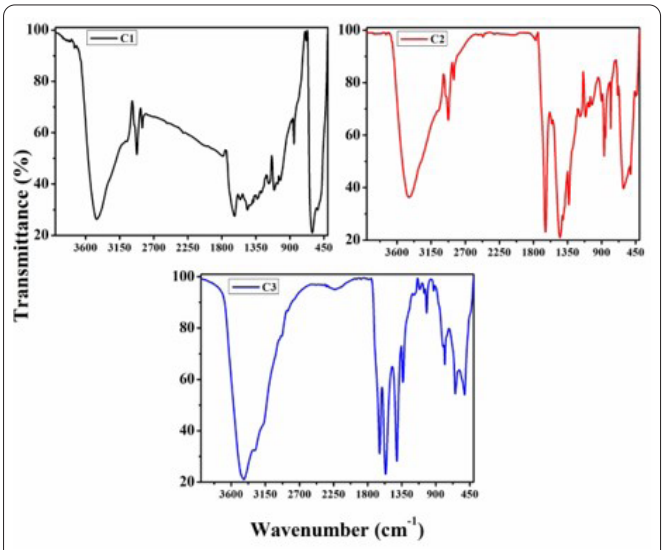


Figure 4: Functional group investigation of Cu_2O nanoparticles.

Table 5: Bond length studies of Cu_2O nanoparticles.

Sample code	Direction	Bond length (Å)
C1	Cu-O	1.8472
	Cu-Cu diagonal	3.0165
	Cu-Cu edge sharing	4.2660
	O diagonal	3.6945
	O-O parallel	4.2660
C2	Cu-O	1.8481
	Cu-Cu diagonal	3.0179
	Cu-Cu edge sharing	4.26979
	O diagonal	3.6961
	O-O parallel	4.2679
C3	Cu-O	1.8481
	Cu-Cu diagonal	3.0179
	Cu-Cu edge sharing	4.2680
	O diagonal	3.6962
	O-O parallel	4.2680

For the bandgap determination $(F(R)h\upsilon)^2$ instead of $(\alpha h\nu)^2$ and plotted. On the other side F(R) also can be considered as K/S ratio, where K is absorption coefficient and S is Scattering coefficient. We have also compared those values. Bandgap and comparison between energy bandgap $(F(R)h\upsilon)^2$ and optical bandgap K/S ratio also illustrated given in figure 5. The prepared Cu_2O nanoparticles have a band gap (Eg) values for the corresponding samples which are listed in table 6.

Bandgap lies within range of 1.38 - 1.42 eV which shows the enhancement of optical properties than bulk Cu_2O. This helps in conductive and catalytic properties such as removal of dyes [15]. Also, some of literatures reports that calculating bandgap from K/S ratio is also considerable as optical bandgap. So, we have compared those values which indicate same regime with minimal difference of 0.2 eV. This shows the accuracy of optical bandgap with energy bandgap. The relation between energy gap and refractive index of semiconductors is proposed by Herve-Vandamme [16]. The Herve-Vandamme relation is explained on the basis of classical oscillatory theory. In this bandgap energy is considered as a constant [16]. The refractive index value can be found using the band gap value through Herve-Vandamme relation given in equation 7.

$$n = \left(1 + \left(\frac{A}{E_g + B}\right)^2\right)^{\frac{1}{2}} \quad (7)$$

Where A and B are constants with values of 13.6 and 3.4 eV, respectively. The refractive index of the prepared Cu_2O nanoparticles is found and tabulated in table 7. Refractive index is decreasing with increasing concentration which helps to fabricate optical devices.

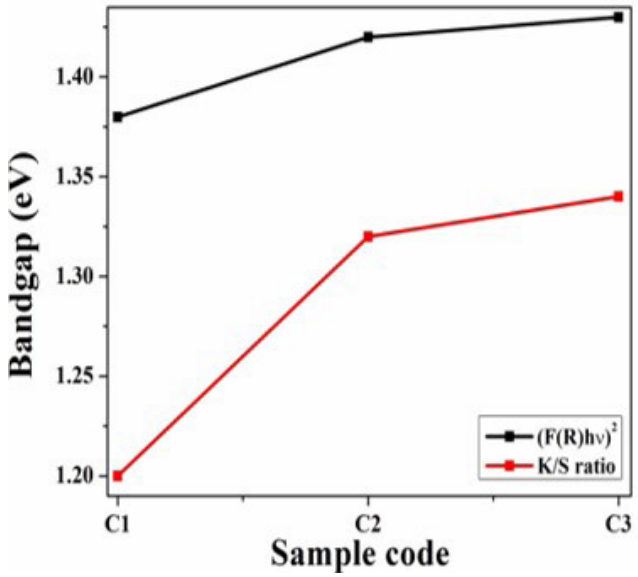


Figure 5: Variation study in optical calculations of Cu_2O nanoparticles.

Table 6: Bandgap studies of Cu_2O nanoparticles.

Sample code	K/S ratio (eV)	$F(R)h\nu^2$ (eV)
C1	1.2	1.38
C2	1.32	1.42
C3	1.34	1.43

Table 7: Optical studies of Cu_2Onanoparticles.

Sample code	Refractive index
C1	3.015
C2	2.993
C3	2.987

Conclusion

Cu_2O nanoparticles were synthesized through precipitation method and morphological, structural, optical properties were studied. This article reports that molar ratio increases the affinity between atoms and strengthens the ionic strength. The properties of the nature are extending and being modified depending upon the molar ratio.

Acknowledgements

None.

Conflict of Interest

None.

References

1. Sharma VP, Sharma U, Chattopadhyay M, Shukla VN. 2018. Advance applications of nanomaterials: a review. *Mater Today Proc* 5(2): 6376-6380. https://doi.org/10.1016/j.matpr.2017.12.248
2. Palani G, Arputhalatha A, Kannan K, Lakkaboyana SK, Hanafiah MM, et al. 2021. Current trends in the application of nanomaterials for the removal of pollutants from industrial wastewater treatment—a review. *Molecules* 26(9): 2799. https://doi.org/10.3390/molecules26092799
3. Raja K, Jaculine MM, Jose M, Verma S, Prince AAM, et al. 2015. Sol-gel synthesis and characterization of α-Fe_2O_3 nanoparticles. *Superlattices Microstruct* 86: 306-312. https://doi.org/10.1016/j.spmi.2015.07.044
4. Rajaeiyan A, Bagheri-Mohagheghi MM. 2013. Comparison of sol-gel and co-precipitation methods on the structural properties and phase transformation of γ and α-Al_2O_3 nanoparticles. *Adv Manuf* 1: 176-182. https://doi.org/10.1007/s40436-013-0018-1
5. Bhanvase BA, Shende TP, Sonawane SH. 2017. A review on graphene–TiO_2 and doped graphene–TiO_2 nanocomposite photocatalyst for water and wastewater treatment. *Environ Technol Rev* 6(1): 1-14. https://doi.org/10.1080/21622515.2016.1264489
6. Ong CB, Ng LY, Mohammad AW. 2018. A review of ZnO nanoparticles as solar photocatalysts: synthesis, mechanisms and applications. *Renew Sustain Energy Rev* 81: 536-551. https://doi.org/10.1016/j.rser.2017.08.020
7. Northey S, Mohr S, Mudd GM, Weng Z, Giurco D. 2014. Modelling future copper ore grade decline based on a detailed assessment of copper resources and mining. *Resour Conserv Recycl* 83: 190-201. https://doi.org/10.1016/j.resconrec.2013.10.005
8. Gu G, Zhu R, Chen Z. 2019. Structural modification of cellulose to enhance the flotation efficiency of fine copper oxide ore. *Physicochem Probl Miner Process* 55(1): 58-69.
9. Han J, Liu W, Xue K, Qin W, Jiao F, et al. 2017. Influence of NH_4HF_2 activation on leaching of low-grade complex copper ore in NH_3-NH_4Cl solution. *Sep Purif Technol* 181: 29-36. https://doi.org/10.1016/j.seppur.2017.03.012

10. Mallik M, Monia S, Gupta M, Ghosh A, Toppo MP, et al. 2020. Synthesis and characterization of Cu_2O nanoparticles. *J Alloys Compd* 829: 154623. https://doi.org/10.1016/j.jallcom.2020.154623
11. Kirfel A, Eichhorn K. 1990. Accurate structure analysis with synchrotron radiation. The electron density in Al_2O_3 and Cu_2O. *Acta Crystallogr Sec A Found Crystallogr* 46(4): 271-284. https://doi.org/10.1107/S0108767389012596
12. Xing W, Meng F, Yu R. 2021. Atomic structure of the Cu_2O (111) surface: a transmission electron microscopy and DFT + *U* study. *Phys Status Solidi* 258(10): 2100185. https://doi.org/10.1002/pssb.202100185
13. Peng B, Zhang S, Yang S, Wang H, Yu H, et al. 2014. Synthesis and characterization of g-C_3N_4/Cu_2O composite catalyst with enhanced photocatalytic activity under visible light irradiation. *Mater Res Bull* 56: 19-24. https://doi.org/10.1016/j.materresbull.2014.04.042
14. Zotov N, Petrov K, Dimitrova-Pankova M. 1990. Infrared spectra of Cu(II)-Co(II) mixed hydroxide nitrates. *J Phys Chem Solids* 51(10): 1199-1205. https://doi.org/10.1016/0022-3697(90)90102-L
15. Guo Y, Dai M, Zhu Z, Chen Y, He H, et al. 2019. Chitosan modified Cu_2O nanoparticles with high catalytic activity for p-nitrophenol reduction. *Appl Surf Sci* 480: 601-610. https://doi.org/10.1016/j.apsusc.2019.02.246
16. Hervé P, Vandamme LKJ. 1994. General relation between refractive index and energy gap in semiconductors. *Infrared Phy Technol* 35(4): 609-615. https://doi.org/10.1016/1350-4495(94)90026-4